

Anisotropic charge displacement supporting isolated photorefractive optical needles

Eugenio DelRe and Alessandro Ciattoni

*Dipartimento di Fisica, Università dell'Aquila, 67100 L'Aquila and
Istituto Nazionale di Fisica Nucleare, Unità di Roma 1, 00185 Rome, Italy*

Aharon J. Agranat

Department of Applied Physics, Hebrew University of Jerusalem, Jerusalem 91904, Israel

Received December 18, 2000

Strong asymmetry in the charge distribution supporting a single noninteracting spatial needle soliton in a paraelectric photorefractive is directly observed by means of electroholographic readout. Whereas in trapping conditions a quasi-circular wave is supported, the underlying double-dipolar structure can be made to support two distinct propagation modes. © 2001 Optical Society of America

OCIS codes: 190.5330, 230.2090.

Far from being a peculiarity of low-dimensional systems, solitary waves and solitons have been widely documented in bulk three-dimensional environments.^{1,2} In biased photorefractives, nonlinear visible optical waves have been shown to undergo self-trapping both as extended one-dimensional waves, in the form of slab solitons,³ and as confined two-dimensional spatial beams, or needle solitons.⁴ Needle solitons are self-funneled micrometer-sized beams of light that propagate through the bulk dielectric without suffering diffraction or distortion. Needles, in their richer higher-dimensional environment, have led to a substantial advance in our phenomenological investigation of nonlinear dynamics, expanding the scope of possible soliton-based applications.

Whereas both slabs and needles emerge from the same physical system, a biased photorefractive sample, their underlying nonlinear nature is rather different.⁵ For slabs, the entire physical system, and thus, consequently, the optical nonlinearity, depends on only the transverse beam direction along which the external field is applied (say the x direction), whereas the system is fully invariant for spatial translations in the second orthogonal transverse direction, y . This reduces slab-soliton description to that associated with a saturated Kerr-like nonlinearity.⁶ For needles, however, the higher dimensionality of the optical beam, whose quasi-circular symmetry suggests an isotropic self-action,⁴ is inherently at odds with the screening nonlinearity, whose one basic driving mechanism is the x -directed external bias field. A simplified description of needles, tracing the steps that lead to a local Kerr-like understanding of slabs, is simply not possible.^{7,8} Given the complexity of the higher-dimensional interaction, the theoretical interpretation of needles is largely based on numerical integration. What emerges is a picture in which nonlocal nonlinear effects,⁹ as opposed to local conventional paradigm Kerr-like phenomenology, play a central role. An understanding of these effects

requires an explicit distinction between the underlying space-charge field distribution E_{sc} , which mediates self-action, and the propagating light field, E_{opt} . The space-charge distribution simply does not have a local relationship to the optical field.⁷ Numerical simulation indicates that the highly anisotropic screening configuration allows the formation of needles only through an equally anisotropic local space charge, characterized by the appearance of two distinct lateral field lobes in the x direction, that are absent in the second transverse direction, y .^{5,9} This double-dipolar field distribution induces, as a consequence, a complicated needle-supporting index pattern that has little to do with a mere self-written graded-index waveguide. For system parameters far from the soliton-supporting configuration, this anisotropy leads to an observable asymmetric beam distortion,^{10,11} but the question naturally arises as to how these lobes manifest their existence when the optical beam is actually a needlelike solitary wave.

Repulsion of mutually incoherent needles provides indirect evidence of the lobelike charge distribution.¹² However, to our knowledge no direct experimental evidence of charge anisotropy has yet been reported. The main reason lies in the fact that photorefractive solitons are generally observed in ferroelectric samples. In these crystals there is no direct way of isolating the contribution of charge displacement from the final guiding structure. Readout with nonphotorefractively active light does not lead to a substantial increase in knowledge of the underlying charge pattern, unless one performs precise bulk interferograms or far-field soliton transforms.^{9,13} Direct investigation of the space-charge residue with a probe is further hampered by the fact that the lobes are actually antiguiding.^{5,9}

In this Letter we give direct evidence of this nonlocal field structure. This is made possible by the quadratic electro-optic response of paraelectrics, which allows the electroholographic separation of optical phenomenology from the underlying space-charge field.¹⁴

Experiments are carried out in a sample of photorefractive $3.7^x \times 4.7^y \times 2.4^z$ mm potassium lithium tantalate niobate,¹⁵ biased along the x axis (of size $L = 3.7$ mm) and kept at a constant temperature $T = 20^\circ\text{C}$. The x -polarized cw TEM₀₀ $\lambda = 532$ nm beam from a diode-pumped double Nd:YAG laser is focused on the input facet of the sample and launched along the z axis. As the beam propagates in the sample, it is diffracted, passing from an initial intensity $I = |E_{\text{opt}}|^2$ FWHM in the x and y directions, $\Delta x \cong \Delta y \cong 10 \mu\text{m}$, to a broadened intensity distribution, $\Delta x \cong \Delta y \cong 20 \mu\text{m}$ [see Figs. 1(a) and 1(b)]. The application of the external constant bias V to the x electrodes makes photoexcited free charges drift, leading to inhomogeneous field screening. The electro-optic response of the paraelectric sample is $\Delta n = -(1/2)n^3 g_{11} \epsilon_0^2 (\epsilon_r - 1)^2 (V/L)^2 [E/(V/L)]^2 \equiv -\Delta n_0 \mathcal{E}^2$, where $n \cong 2.4$ is the zero-field index of refraction, $g_{11} \equiv g_{xxxx} \cong 0.12 \text{ m}^4 \text{ C}^{-2}$ is the dominant component of the quadratic electro-optic tensor g_{ijkl} (and thus tensorial effects are neglected), ϵ_0 is the vacuum dielectric constant, $\epsilon_r \cong 9 \times 10^3$ (at $T \cong 20^\circ\text{C}$) is the relative sample's low-frequency dielectric constant, E is the x component of the electric field resulting from screening, $\Delta n_0 \cong 2.8 \times 10^{-4}$, and $\mathcal{E} \equiv E/(V/L)$. The spatially modulated index distribution allows needle formation [see Fig. 1(c)]. The needle, which allows a slight anisotropy in the output intensity distribution, is trapped and stable in time for an external bias voltage of $V = 0.85$ kV and a ratio of peak intensity I_p to the dark artificial illumination I_b (obtained by illumination of the sample with a copropagating y -polarized plane wave of equal wavelength) of $u_0^2 \equiv I_p/I_b \cong 2.6$. Annulling the externally applied voltage V , i.e., setting $V = 0$, gives an index modulation, $\Delta n_{V=0} = -\Delta n_0 \mathcal{E}_{\text{sc}}^2$, that is due only to the charge displacement, where evidently $\mathcal{E}_{\text{sc}} \equiv \mathcal{E} - 1$. The resulting index pattern has a guiding structure for regions in which \mathcal{E}_{sc} passes through a minimum. Given that the lobes represent an excess of screening in the x direction,^{5,9} there are two points, i.e., x_1 and x_2 , along the x axis, located to the left and right of the needle peak, respectively, in which $\Delta n_{V=0}$ forms a guiding hump. Along the y axis, this hump will follow the shape of the lobe.

To investigate $\Delta n_{V=0}$ without modifying the space-charge distribution, we launch into the sample the same beam that leads to the needle but attenuated to have a much lower intensity. This attenuation guarantees that the characteristic time scale of charge displacement induced by the probe, τ_d , is much longer than any characteristic observation time. For typical microwatt-intensity beams, $\tau_d \sim 1$ min.

The results, shown in Fig. 1(d), clearly indicate an anisotropic lobe structure in the form of a split diffraction pattern in the x direction. The slight asymmetry in the diffraction pattern is a consequence of needle self-bending, which inevitably distorts the diffractive readout phase. In this study we have also observed a similar phenomenology for transient quasi-steady-state needles, where $I_b = 0$, blocking beam evolution in the trapped regime, i.e., before the needle has decayed.

The two light lobes constitute direct proof that the nonlinearity that supports needle trapping in biased photorefractives is not the saturated Kerr-like electro-optic response, $\Delta n \propto 1/(1 + I/I_b)^2$, that allows slab formation. More precisely, whereas the lobes are not present in the slab case (and are not merely negligible), they play a fundamental role in needle trapping.¹⁶ Although needles have been documented in various conditions, it is legitimate to ask whether the nonlocal space-charge field structure, and thus the index modulation, can actually support circular-symmetric solitary waves, given that the most general manifestation is strong transient oscillatory behavior.⁸ The mathematical answer is no.¹⁷ However, the anisotropic space-charge structure can support waves that are for all practical purposes circular symmetric and nonoscillating. For the conditions investigated experimentally, we find the space-charge distribution by solving the simplified associated electrostatic problem, i.e., $\nabla \cdot [(I + I_b)\mathbf{E} + (K_b T/q)\nabla I] = 0$,⁷ where \mathbf{E} is the internal electric field vector, starting from the experimental input Gaussian intensity distribution. The resulting index pattern is shown in Fig. 2(a). Propagating the same field distribution E_{opt} [whose intensity I is shown in Fig. 2(b)] into this pattern gives the results shown in Figs. 2(c) and 2(d). The intensity pattern does not suffer discernible distortion, apart from a small constant oscillation (see the caption of Fig. 2). This lack of distortion means that the exact nonlinear behavior, restricted to our experimental configuration, is well described by this approximate linear approach, and thus we can

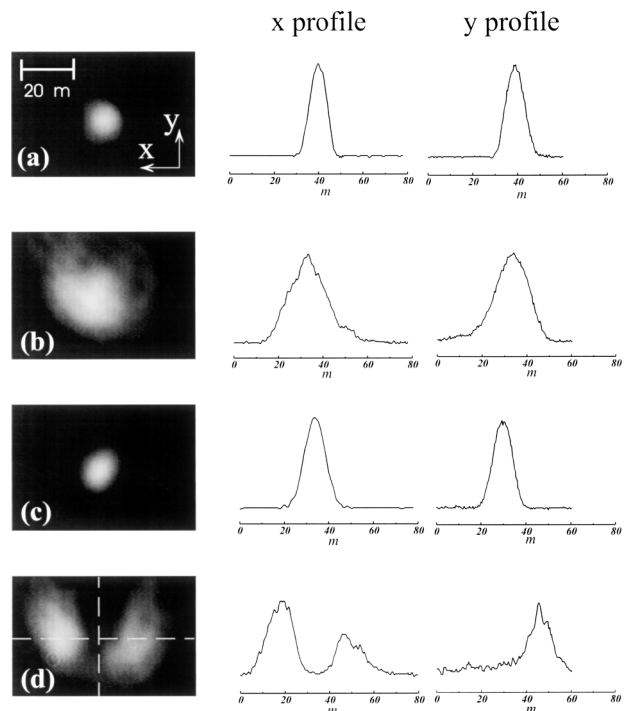


Fig. 1. Electroholography of a single photorefractive needle: (a) Image and profiles of input transverse intensity distribution, (b) linear diffraction with nonlinear charge separation turned off ($V = 0$), (c) self-trapping distribution for $V = 0.85$ kV, (d) readout for $V = 0$.

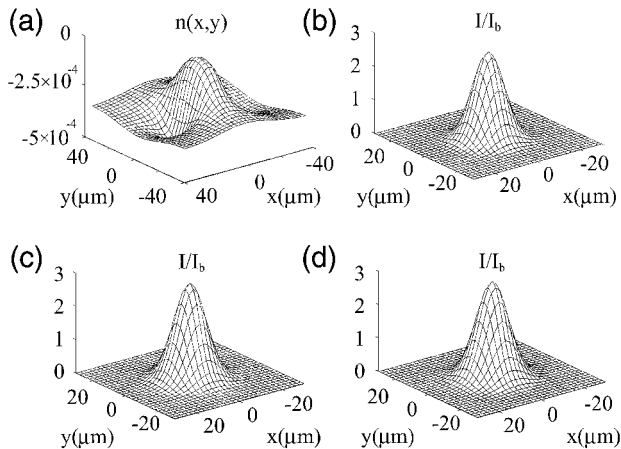


Fig. 2. Self-consistency of needle solitons trapped in an anisotropic nonlinear index pattern: (a) anisotropic index pattern, (b) input intensity distribution, (c), (d) intensity after (c) 4.5- and (d) 25-mm (i.e., ~ 18 diffraction lengths) propagation, respectively, for the experimental situation described above. Throughout propagation the asymmetric oscillatory behavior was stable, such that $|\Delta x/\Delta y - 1| < 1\%$.

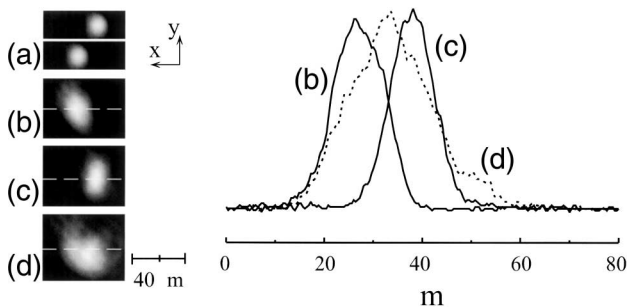


Fig. 3. Double-hump guiding structure: (a) Two different input beams, shifted by approximately $\pm 10 \mu\text{m}$, (b), (c) guided beam in the two humps, (d) linear diffraction of the unshifted beam.

conclude that quasi-circular needles can be supported by the anisotropic pattern.¹⁸

One basic consequence of these findings is that the anisotropy underlying a photorefractive needle leads not to one but to three spatially separated index structures that can be made to alternatively guide light, depending on the applied external voltage in the readout phase. This consequence would not have been possible had the nonlinear response been local, as in the one-dimensional case.¹⁴ The electroholographic readout would have implied a transition from a localized single-mode structure (the needle) to a delocalized doughnutlike guiding pattern. To demonstrate this transition we investigate the guiding capabilities at $V = 0$. We were able to show the two guided modes launching, in sequence, the probe beam

into one of the two lateral guiding humps of the $\Delta n_{V=0}$ pattern, i.e., in x_1 and x_2 . The results are shown in Fig. 3. We did not observe any directional coupling between the modes, which was clearly a consequence both of the distances between the humps, the probe wavelength, and the propagation length and of the presence of the antiguiding central pattern.

This study was funded by the Italian Istituto Nazionale Fisica della Materia through the PAIS2000 Soliton-based electro-optic structures in near-transition photorefractive crystals and bulk optical manipulation (SESBOM) project. Research carried out by A. J. Agranat is supported by a grant from the Ministry of Science of the State of Israel. E. DelRe's e-mail address is edelre@libero.it.

References

1. G. I. Stegeman and M. Segev, *Science* **286**, 1518 (1999).
2. M. Segev and M. Stegeman, *Phys. Today* **51**(8), 42 (1998).
3. M. Segev, B. Crosignani, A. Yariv, and B. Fischer, *Phys. Rev. Lett.* **68**, 923 (1992).
4. M. Shih, M. Segev, G. C. Valley, G. Salamo, B. Crosignani, and P. Di Porto, *Electron. Lett.* **31**, 826 (1995).
5. A. A. Zozulya and D. Z. Anderson, *Phys. Rev. A* **51**, 1520 (1995).
6. M. Segev, M. Shih, and G. C. Valley, *J. Opt. Soc. Am. B* **13**, 706 (1996).
7. B. Crosignani, P. Di Porto, A. Degasperis, M. Segev, and S. Trillo, *J. Opt. Soc. Am. B* **14**, 3078 (1997).
8. A. A. Zozulya, D. Z. Anderson, A. V. Mamaev, and M. Saffman, *Europhys. Lett.* **36**, 419 (1996).
9. C. M. Gómez Sarabia, P. A. Márquez Aguilar, J. J. Sánchez Mondragón, S. Stepanov, and V. Vysloukh, *J. Opt. Soc. Am. B* **13**, 2767 (1996).
10. G. S. Garcia Quirino, M. D. Iturbe Castillo, J. J. Sánchez Mondragón, S. Stepanov, and V. Vysloukh, *Opt. Commun.* **123**, 597 (1996).
11. N. Korneev, P. A. Márquez Aguilar, J. J. Sánchez Mondragón, S. Stepanov, M. Klein, and B. Wechsler, *J. Mod. Opt.* **43**, 311 (1996).
12. W. Krolikowski, M. Saffman, B. Luther-Davies, and C. Denz, *Phys. Rev. Lett.* **80**, 3240 (1998).
13. One-axis interferometry such as that described in Ref. 10 cannot be used here because in the highly localized case of needles the beams are self-bending.
14. E. DelRe, M. Tamburrini, and A. J. Agranat, *Opt. Lett.* **25**, 963 (2000).
15. A. J. Agranat, R. Hofmeister, and A. Yariv, *Opt. Lett.* **17**, 713 (1992).
16. There is no fundamental difference between anisotropy in paraelectrics and ferroelectrics.
17. M. Saffman and A. A. Zozulya, *Opt. Lett.* **23**, 1579 (1998).
18. This approach differs from those reported in previous studies in that it is greatly simplified but, consequently, can only be used to confirm or contradict our specific experimental results.